Florian Schlüter, Johannes Meyer, Michaela Wilhelm, Kurosch Rezwan

Hierarchical emulsion based hybrid ceramics synthesized with different siloxane precursor and with embedded nickel nanoparticles

Journal Article as: peer-reviewed accepted version (Postprint)

DOI of this document*(secondary publication): 10.26092/elib/2482

Publication date of this document: 22/09/2023

* for better findability or for reliable citation

Recommended Citation (primary publication/Version of Record) incl. DOI:

Florian Schlüter, Johannes Meyer, Michaela Wilhelm, Kurosch Rezwan,
Hierarchical emulsion based hybrid ceramics synthesized with different siloxane precursor and with embedded nickel nanoparticles,
Colloids and Surfaces A: Physicochemical and Engineering Aspects,
Volume 492, 2016, Pages 160-169, ISSN 0927-7757,
https://doi.org/10.1016/j.colsurfa.2015.12.020.

Hierarchical emulsion based hybrid ceramics synthesized with different siloxane precursor and with embedded nickel nanoparticles

Florian Schlüter, Johannes Meyer, Michaela Wilhelm *, Kurosch Rezwan

University of Bremen, Advanced Ceramics, Am Biologischen Garten 2, D-28359 Bremen, Germany

GRAPHICAL ABSTRACT

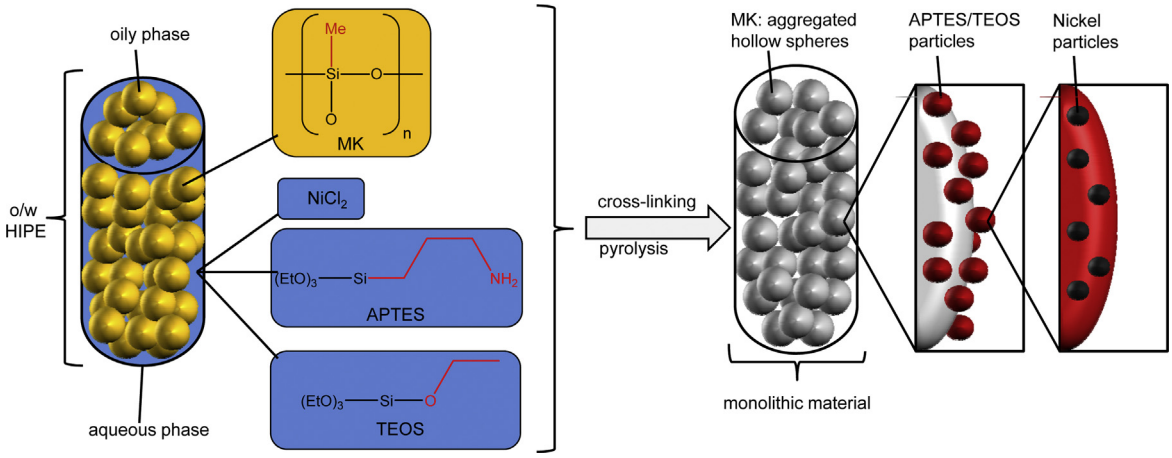

HIGHLIGHTS

- Hybrid ceramics with hierarchical pore size distribution.
- Tunable surface characteristics and pore size distribution.
- High content of different organic groups (>75 mol-%) in cross-linked precursor.
- Generation of Ni containing materials by using embedded APTES as complexing agent.

ARTICLE INFO

Article history:
Received 3 July 2015
Received in revised form
10 December 2015
Accepted 18 December 2015
Available online 23 December 2015

Keywords:
Hybrid ceramics
Surface characteristics
Porosity
Monolithic material
Emulsion

* Corresponding author. Fax: +49 421 218 64932.
E-mail address: mwilhelm@uni-bremen.de (M. Wilhelm).

http://dx.doi.org/10.1016/j.colsurfa.2015.12.020

ABSTRACT

An emulsion-based synthesis route for the generation of organo-silica-based monolithic hybrid ceramics with a high content of different organic groups and embedded nickel nanoparticles is presented. By this route hybrid ceramics with a hierarchical pore size distribution and tailorable surface characteristics can be obtained. Mixtures of methyl polysiloxane (MK), tetraethyl orthosilicate (TEOS) and (3-aminopropyl)triethoxysilane (APTES) with varying ratios are selected as precursors, cross-linked, and subsequently pyrolyzed at 500 or 600 °C. In this way monolithic emulsion based hybrid ceramics with three different organo-functionalized siloxane precursor can be synthesized. Additionally, by adding the metal precursor $NiCl_2$, metal-containing emulsion-based hybrid ceramics can be achieved. By adjusting the oil/water ratio and using high- or low internal phase emulsions (HIPEs or LIPEs), controlled micro-, meso-, and macropore distributions are obtained. After pyrolysis, materials achieve specific BET surface areas of up to 550 m^2/g. Adjustable surface characteristics in terms of hydrophobicity and hydrophilicity of the material surface by thermal decomposition behavior of precursors is demonstrated.

Nickel is incorporated through the formation of complexes with APTES, resulting in well-distributed metal nanoparticles with average particle sizes between 35 and 69 nm. The material properties are pivotal features for catalysis and gas separation applications.

1. Introduction

Polymer-derived ceramics (PDCs) are an important target for current ceramics research, largely due to their low-cost synthesis and numerous forming and shaping possibilities. Polysiloxane-based, hierarchically-ordered materials with different functional organic groups are extremely versatile, with many possible applications: as high-temperature-resistant materials for energy, aerospace, or automotive purposes; hard materials; chemical engineering materials for catalyst support structures or biotechnological purposes; or functional materials in electrical engineering, including micro- and nanoelectronics [1–4]. Hybrid ceramics, also called ceramers, are a sub-group of PDC materials [5], with properties that reflect both ceramic and polymeric characteristics [6]. Ceramers may be obtained by pyrolysis of polysiloxane precursors under an atmosphere of nitrogen at temperatures between 400 and 800 °C. SiOC ceramics will be formed at pyrolysis temperatures between 800 and 1200 °C, and crystalline SiC will be generated at pyrolysis temperatures higher than 1200 °C. Partial decomposition of the organic moieties at temperatures between 400 and 600 °C develops a pronounced microporosity in the ceramers, resulting in specific surface areas as high as 700 m^2/g [7].

Adjustments of important PDC surface characteristics (hydrophobicity/hydrophilicity, pore size distribution, and specific surface area) are made possible by modifying the pyrolysis temperatures, precursor compositions, and reaction conditions. Polysiloxane precursors are easily formed at the macroscopic scale, in addition to numerous smaller-scale tailorable pore shape characteristics [8–11]. These very controllable form factors allow for adjustments that improve their mechanical stability, making them excellent candidates for use in mass transport-limited catalysis processes.

Previous work in the author's research group has demonstrated that ceramers with metal nanoparticles (Ni(II), Pt(IV)) can be generated by using APTES as a complexing agent at pyrolysis temperatures between 400 and 600 °C. These materials can generally be prepared in a simple one-batch synthesis, whereby porosity and surface characteristics can be adjusted by varying the siloxane precursors. In addition, there are first results indicating a more homogeneous distribution of metallic particles throughout the matrix if complexing siloxanes are incorporated as precursor [9,12,13].

However, metallic components can be homogenously distributed in a silica matrix by using organo-functionalized siloxanes. These silxoanes are able to form complexes with metal ions, incorporating metallic components into the matrix [14–16]. By an oxidative removal of the organic groups, metal particles can be generated in silica microspheres [15]. The size of the resultant metal nanoparticles is dependent upon various parameters; for example, nickel nanoparticles show a strong dependency on the nickel salt as metal precursor. Particles in a range from 3 to 82 nm are observed. $Ni(NO_3)_2$, $Ni(OAc)_2$, $NiCl_2$ and $Ni(acac)_2$ were investigated. Smaller particles were received for $Ni(NO_3)_2$ and $Ni(OAc)_2$, bigger particles for $NiCl_2$ and $Ni(acac)_2$ [17].

For applications in catalysis, a hierarchical porosity is very important. A promising template method for creating hierarchical structures is emulsion-based synthesis. In particular, high internal phase emulsions (HIPEs) are a promising class of emulsions in sol–gel processing [3,18,19]. Although the HIPE process has been intensively studied for organic polymers, it has only rarely been used with polysiloxane precursors [20–26]. HIPEs are defined by an internal phase volume fraction higher than 74% of the total emulsion volume. If the internal phase volume is lower than 26%, the emulsions are called low internal phase emulsions (LIPEs) [27]. The droplets in HIPEs are usually separated by a thin film of the continuous phase [2,3]. The first polymer foams prepared with HIPEs were published in the 1960s [28]. These so-called "poly-HIPEs" are prepared by polymerizing the continuous phase, the internal phase, or both. Polymerization of the continuous phase usually leads to the formation of porous materials with a foam-type structure. In contrast, polymerization of the internal phase usually results in an aggregated hollow sphere structure [29]. Surfactant choice is of primary importance; it will decide whether an oil-in-water (o/w) or water-in-oil (w/o) emulsion will form, depending on the Bancroft rule [30] or the hydrophilic-lipophilic balance [31].

After the first synthesis of macroporous silica monoliths in 1998 with a combination of an o/w emulsion and a sol–gel processing by Imhof and Pine [26], further developments were made by Backov et al. [21–25]. These pioneering workers in the synthesis of macroporous silica monoliths from o/w emulsions have been able to generate silica-based monolithic materials with hierarchical porosities (labeled Si(HIPE)). These materials were generated by dissolving tetraethyl orthosilicate (TEOS) as a precursor in the continuous phase. It is also possible to add organic-functionalized monomeric siloxanes to TEOS – such as phenyltriethoxysilane, methyltriethoxysilane, or *N*-(3-trimethoxysilylpropyl) pyrrol – in amounts of up to 20 wt%. Previous workers have labeled these materials "R-Si(HIPE)s" or "organo-Si(HIPE)s" [22]. These monolithic R-Si(HIPE) s show macropores with accessible micro- and mesoporosities [22,23,32]. However, using concentrations of R-$Si(OEt)_3$ higher than 20 wt% generates powders instead of monolithic materials. Besides direct incorporation of functional groups, post-synthesis functionalization of a TEOS-based Si(HIPE) support is also possible [25]. Metal-containing R-Si(HIPE) s have been generated by using an adsorption/complexing process of metal salts from aqueous solution (e.g. Eu or Pd) [23,32,33].

Previously works of our group showed that the generation of monolithic emulsion based ceramers, (MEBC) which were obtained by using HIPE, MIPE (medium internal phase emulsions) or LIPE processes, starting with silica precursor, which exhibits only methyl and/or phenyl groups (MK and H44) are possible. The tailoring of the macroscopic structure was possible by using different kinds of emulsions (HIPEs, MIPEs or LIPEs). Additionally, controllable micro and macropore distributions with cell windows in a range between 2 and 50 nm for hollow spheres are obtained. Tailoring of the surface characteristics in terms of hydrophobicity/hydrophilicity is possible by precursor selection, using a methyl and phenyl group containing precursor or a precursor with only methyl groups in different ratios. The pyrolysis of different precursor composition at 500 or 600 °C results in specific BET surface areas up to 600 m^2/g without losing the monolithic structure.

The authors will refer to materials produced by the emulsion processes as "monolithic emulsion-based ceramers" (MEBC). The main goal of this study was to synthesize MEBCs with different

polysiloxane precursor and with that materials which show in the cross-linked state a high content of different organic groups (>75 mol-%) in order to tailor the material properties specifically. Additionally, materials containing Ni nanoparticles, using APTES as the complexing agent, were synthesized in order to generate catalytic active materials. In pursuit of this goal, the authors examine different pore morphologies, surface characteristics, and specific surface areas of polysiloxane-derived MEBCs after pyrolysis at 500 or 600 °C.

2. Material and methods

2.1. Preparation

MEBCs were prepared from methyl polysiloxane (Silres® MK, Wacker Chemie AG) and a monomer: either tetraethyl orthosilicate (TEOS; Sigma–Aldrich Co., LLC), or (3-aminopropyl) triethoxysilane (APTES; ABCR Dr. Braunagel GmbH & Co. KG). $NiCl_2$ (Sigma–Aldrich Co., LLC) was used as the metallic precursor. Specific ratios for each compound are given in Table 1. To create the emulsion, an oily phase and an aqueous phase were first prepared separately. The oily phase was prepared by dissolving MK in 4 ml of toluene (ABCR Dr. Braunagel GmbH & Co. KG) to produce either a 12 M solution (for samples without Ni), or a 9 M solution (for samples containing Ni). The aqueous phase was prepared by dissolving varying amounts of APTES, TEOS, and $NiCl_2$ in an NH_3 solution (see Table 1). In order to cause the oily phase to act as the internal phase and the aqueous phase to act as the continuous phase, the surfactant tetradecyltrimethylammonium bromide (TTAB 35 wt-%; ABCR Dr. Braunagel GmbH & Co. KG) was added to the aqueous phase.

To prepare the different o/w emulsions, the phase with the higher volume was added to the other phase drop by drop under stirring at 500 rpm HIPE (internal phase volume >74%) and LIPE (internal phase volume <26%) [27]. The reaction vessel was sealed and the emulsions were allowed to cross-link for 5 days at room temperature, catalyzed by NH_3. After one or two minutes, depending on the composition, a white monolithic solid were formed from the emulsions. After decanting the solvent, the solid was dried 20 °C. This was followed by additional drying and cross-linking steps given in Fig. 1. The final step was carried out in vacuum (~2 mbar) for 5 h at 150 °C. The vacuum process at 150 °C was performed in order to remove toluene and water, in addition to a final thermal cross-linking step. Lastly, the specimens were pyrolyzed at either 500 or 600 °C in an atmosphere of nitrogen. A heating rate of 120 °C/hour was used up to 100 °C below the final temperature and then a heating of 30 °C/h were applied to avoid overheating. The specimens were pyrolyzed at the maximal temperature for 4 h. After pyrolysis, samples based on pure MK were white in color. APTES- and TEOS-containing samples had a brownish color post-pyrolysis, visually indicating a higher degree of precursor decomposition. Pyrolysis of the greenish Ni-containing cross-linked samples resulted in black monolithic structures (Fig. 1c).

For samples based on pure MK the denotation is as follows: the used precursor is mentioned first, the oil/water ratio and the pyrolysis temperature in degree Celsius as xxx follow. The denotation of APTES and TEOS containing samples is similar, but A is added for APTES and T for TEOS. The numbers following A and T indicate the molar ratio applied. To give an example, MK-74-A2T1-500 was prepared from MK, APTES and TEOS in a ratio of 10:2:1 (mol-%) with an oil/water ratio of 74/26 (vol.%). The pyrolysis was done at 500 °C. The additional specification Ni indicates that the samples contain Nickel.

The sample set was divided into three subsets. In the first subset, LIPE samples based on MK, APTES, and TEOS were produced to analyze the influence of different precursor compositions on surface characteristics. The ratio of oily internal phase to aqueous continuous phase was held constant. Amounts of APTES and TEOS were varied in the aqueous continuous phase by amounts shown in Table 1. In the second subset, HIPE samples were prepared with the same precursor compositions used in the first (LIPE) subset in order to see the influence of the different emulsion types on the macroscopic structure of the monoliths. In the third subset, the Ni precursor was finally added to the aqueous phase of a HIPE to prepare Ni-containing HIPE, utilizing the same ratios of MK, APTES, and TEOS chosen for the first two subsets. The concentration of the MK precursor was lower compared to Ni-free samples, because the solubility of the Ni-APTES complex in the aqueous phase is limited. For the purpose of comparison, a Ni-free sample with the same precursor concentration was generated (9-MK-74-A2T2-xxx).

2.2. Characterization

According to IUPAC notation, microporous materials have pore diameters of less than 2 nm and macroporous materials have pore diameters of greater than 50 nm. Mesoporous materials have pore diameter in a range from 2 to 50 nm [34]. The macrostructure was analyzed by SEM(20 kV; Camscan Series 2, Obducat CamScan Ltd.). For this purpose, the samples were embedded in a two-component epoxy resin, polished with SiC paper, and sputtered with gold (K550, Emitech, Judges Scientific plc.). Size and distribution of Ni particles in the material was analyzed by TEM (TITAN 80/300 G1, FEI). TEM samples were finely ground and placed dry on TEM grids. The average particle sizes and size ranges were determined by measuring more than 50 nanoparticles found in arbitrarily chosen areas of the TEM images. Mercury intrusion was used to determine the macroporosity (Pascal 140/440, POROTEC GmbH) of the MEBCs. The specific BET surface area was determined by nitrogen adsorption at −196 °C (Belsorp-Mini, Bel Japan Inc.) after grinding and sieving (mesh size 300 μm) to diminish limitation of nitrogen diffusion within the timeframe of the experiment. Finally, the surface characteristics of these sieved powder fractions were investigated by isothermal water and *n*-heptane vapor sorption experiments at 22 °C, recording adsorption-desorption isotherms (Belsorp18-3, Bel Japan Inc.).

3. Results

Preparation of MEBC and Ni-MEBC was done with siloxane precursors, which exhibit methyl and aminopropyl and ethoxy groups by using HIPEs or LIPEs. The introduction of organic groups was done with the polysiloxane MK and APTES as precursors. A total amount of >75 mol-% of organic functionalized precursor were realized in the cross-linked state. The resultant monolithic material is shown in Fig. 1, and all samples exhibited acceptable handling stability during the experimentation process.

3.1. Characterization at the macro and mesoscopic length scale and of the nickel nanoparticles

The type of emulsion used (HIPE or LIPE) strongly affected the samples' macroscopic structural morphologies. Additionally, the introduction of APTES, TEOS, and $NiCl_2$ further modify the macroscopic structures (Fig. 2).

Pure MK-containing samples prepared with HIPEs and LIPEs developed a structure composed of aggregated spheres (Fig. 2a,c). The LIPE samples show a continuous range of sphere sizes (5–25 μm), while the HIPE samples show a somewhat smaller range and overall size of spheres (1–10 μm). The most homogenous structure was observed in sample MK-74-500 (Fig. 2c). Spheres in several

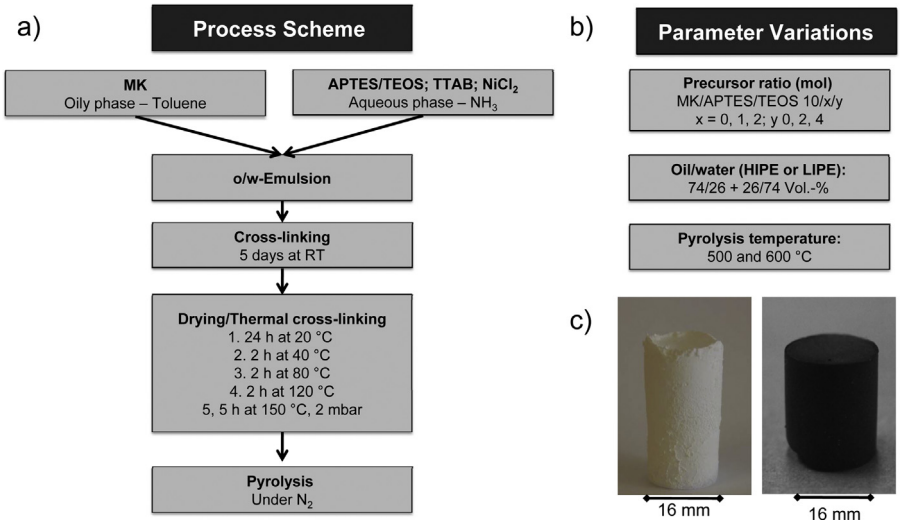

Fig. 1. (a) Process scheme; (b) parameter variation of synthesized samples and (c) monolithic structure of pyrolyzed samples (left without nickel, right with nickel).

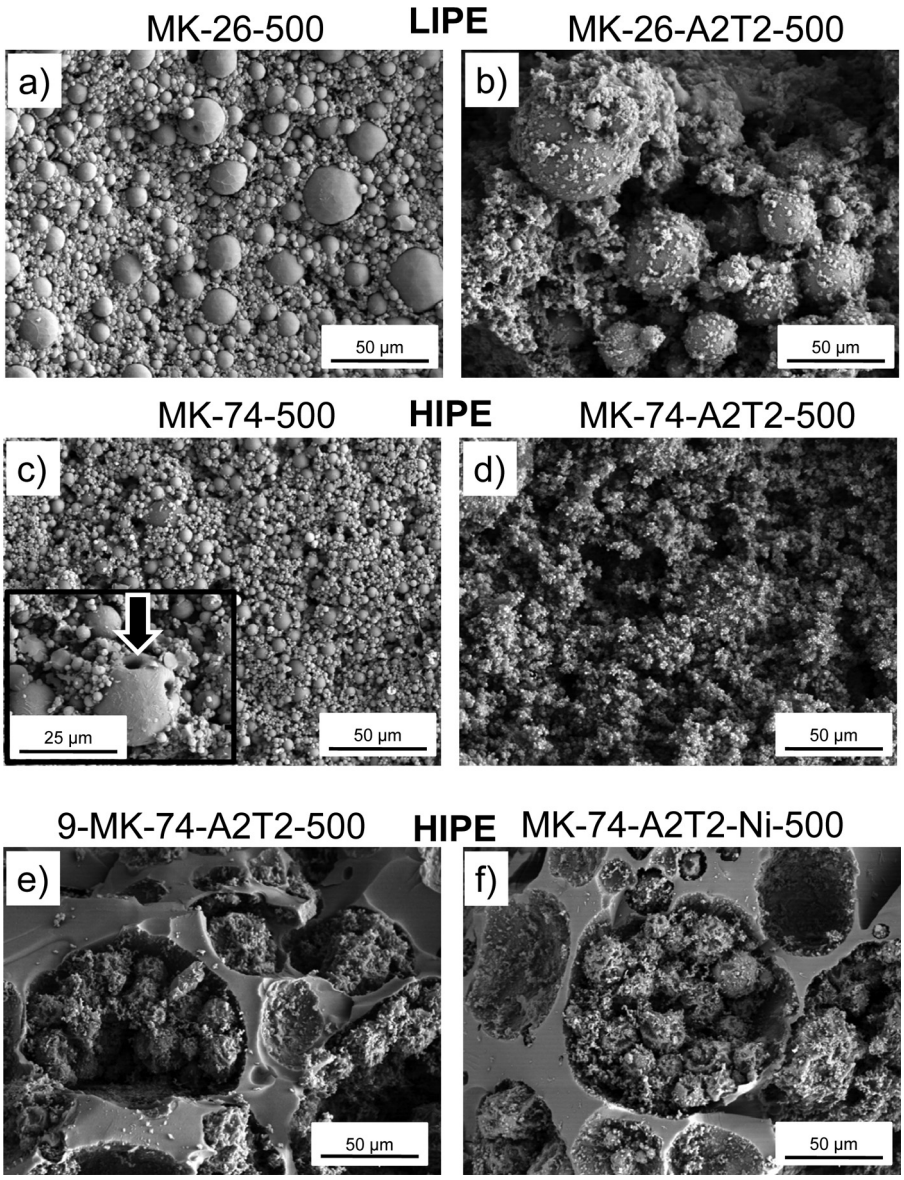

Fig. 2. SEM images of pyrolyzed monoliths with different oil/water ratios and different precursor ratios (a, b: LIPE samples, c–f: HIPE samples). Inset in c shows that spheres are probably hollow.

Table 1
Prepared Materials and their composition, process and pyrolysis parameters. "xxx" refers to the pyrolysis temperature for the sample (500 or 600 °C).

Material denotation	Conc. MK in oily phase (mol/l)	Ratio of MK/APTES/TEOS (mol-%)	Nickel content[a]; related to MK (mol-%)	Oil/water ratio (vol.%)	Conc. of NH_3 (mol/L)	Pyrolysis temperature (°C)
MK-26-xxx	12	10/-/-	–	26/74, LIPE	0.2	500/600
MK-26-A1T1-xxx	12	10/1/1	–	26/74, LIPE	0.2	500/600
MK-26-A2T1-xxx	12	10/2/1	–	26/74, LIPE	0.2	500/600
MK-26-A2T2-xxx	12	10/2/2	–	26/74, LIPE	0.2	500/600
MK-26-A2T4-xxx	12	10/2/4	–	26/74, LIPE	0.2	500/600
MK-74-xxx	12	10/-/-	–	74/26, HIPE	0.2	500/600
MK-74-A1T1-xxx	12	10/1/1	–	74/26, HIPE	0.2	500/600
MK-74-A2T1-xxx	12	10/2/1	–	74/26, HIPE	0.02	500/600
MK-74-A2T2-xxx	12	10/2/2	–	74/26, HIPE	0.02	500/600
MK-74-A2T4-xxx	12	10/2/4	–	74/26, HIPE	0.02	500/600
MK-74-A1T1-Ni-xxx	9	10/1/1	1.25	74/26, HIPE	0.2	500/600
MK-74-A2T1-Ni-xxx	9	10/2/1	2.50	74/26, HIPE	0.2	500/600
MK-74-A2T2-Ni-xxx	9	10/2/2	2.50	74/26, HIPE	0.2	500/600
MK-74-A2T4-Ni-xxx	9	10/2/4	2.50	74/26, HIPE	0.2	500/600
9-MK-74-A2T2-xxx	9	10/2/2	–	74/26, HIPE	0.2	500/600

[a] Nickel/APTES molar ratio 1/8.

Table 2
Average size and size range of Ni particles in samples pyrolyzed at 500 and 600 °C.

Sample	Average particle size [nm]	Size range of particle [nm]
MK-74-A1T1-Ni-500	291	50–800
MK-74-A2T1-Ni-500	462	80–1000
MK-74-A2T2-Ni-500	587	400–1000
MK-74-A2T4-Ni-500	77	10–400
MK-74-A1T1-Ni-600	35	5–200
MK-74-A2T1-Ni-600	69	10–400
MK-74-A2T2-Ni-600	47	10–200
MK-74-A2T4-Ni-600	37	10–200

samples were observed to be at least partially hollow (MK-74-500 shown in Fig. 2c).

The introduction of APTES/TEOS (Fig. 2b,d) leads to residual decomposition products of APTES and TEOS "clinging" to the surfaces of the MK spheres (MK-26-A2T2-500; Fig. 2b).

The use of lower precursor concentrations in the solution (9 mol/L MK; for incorporation of Ni) results in a different macrostructure, compared to the samples prepared with 12 mol/L MK (Fig. 2a–d). It consists of aggregated MK spheres with the residual surficial APTES/TEOS decomposition products embedded in a larger foam-like [super]structure with pore sizes on the order of ~250 μm (Fig. 2e,f). This macrostructure occurs in all samples prepared with 9 mol/L MK—with and without Ni.

Prior to pyrolysis, the samples' macroscopic morphology was investigated by SEM analysis (not shown). These morphologies showed the same macroscopic texture as the pyrolyzed samples. This demonstrates that the formation of the macropores in the samples occurs as a result of the emulsification process, and is not related to the pyrolysis of the samples.

In order to investigate the particle size and distribution of Ni particles, TEM investigations of very fine ground samples were performed. Selected samples are shown in Fig. 3, with average particle sizes and ranges given in Table 2.

For all Ni-MEBCs prepared with a pyrolysis temperature of 500 °C, Ni particles with an unexpectedly diameter were found. Average particle sizes were found to range from 291 to 587 nm. The only exception was MK-74-A2T4-500, shown in Fig. 3b; this material was found to have an average Ni particle size of 77 nm. For all of the samples pyrolyzed at 600 °C, nanoparticles were observed to have smaller average particle sizes (35–69 nm), independent of APTES and TEOS amount and nickel content in the different samples.

Additionally, the samples pyrolyzed at 600 °C and MK-74-A2T4-Ni-500 show a more homogenous distribution of the Ni nanoparticles, shown clearly in Fig. 3. Mercury porosimetry was employed to further characterize details of the macro- and mesoporosities. It should be noted that mercury porosimetry provides information only on the size of the "windows" that connect two adjacent macropores, not the macropore diameters themselves, in the case of the aggregated hollow sphere structure. In Fig. 4a–c, the open porosity and the relative pore volume vs. pore diameter distribution of selected samples are depicted.

In Fig. 4a and b, the meso- and macropore size distributions are shown for samples with different oil/water ratios and amounts of APTES/TEOS pyrolyzed at 500 °C. Adjustment of macropore sizes is possible by using adjusted oil/water ratios. The LIPE samples (Fig. 4a) display a broad monomodal pore size distribution between 1 and 10 μm. Generally, high open porosities of 50–80% were observed. In contrast to the LIPE samples, the HIPE samples show a more bimodal pore size distribution (Fig. 4b). The main diameters are around 0.01 μm and 4 μm. An increasing open porosity (from 20 up to 80%) with increasing APTES/TEOS amounts is observed. Consequently, the LIPE samples show a macroporous structure and the HIPE samples show a macro/meso porous structure. For both sample types, the introduction of APTES/TEOS does not lead to changes in the pore size distribution, compared to the purely MK-containing samples (Fig. 4a and b). Samples pyrolyzed at 600 °C (not shown here) exhibited the same pore size distributions as comparable samples pyrolyzed at 500 °C.

In Fig. 4c, the pore size distribution of selected Ni-MEBCs and 9-MK-74-A2T2-500, pyrolyzed at 500 °C, are depicted. The Ni-HIPE samples show a broad pore size distribution, between 0.004 and 0.2 μm; smaller overall than the Ni-free HIPE samples. The second average cell size expected from SEM cannot be detected by this method. This is in agreement with the above-mentioned SEM analysis (Fig. 2f), which demonstrated already that aggregated spheres are embedded in big pores (up to 250 μm). This pore size distribution is similar to that of the corresponding materials without Ni, which were also synthesized with a MK concentration of 9 mol/L (Fig. 2e). The concentration of the MK solution is responsible for the changes in the pore size distribution; not the incorporation of Ni.

To conclude the mercury intrusions results, a tailoring of pore size distribution using different emulsion types is possible. Only small influences on the pore size distribution are detected for the introduction of APTES/TEOS in Ni-free samples. Pore size distribution changes dramatically for the Ni-HIPE samples as a result of different MK concentrations; in agreement with the SEM analysis.

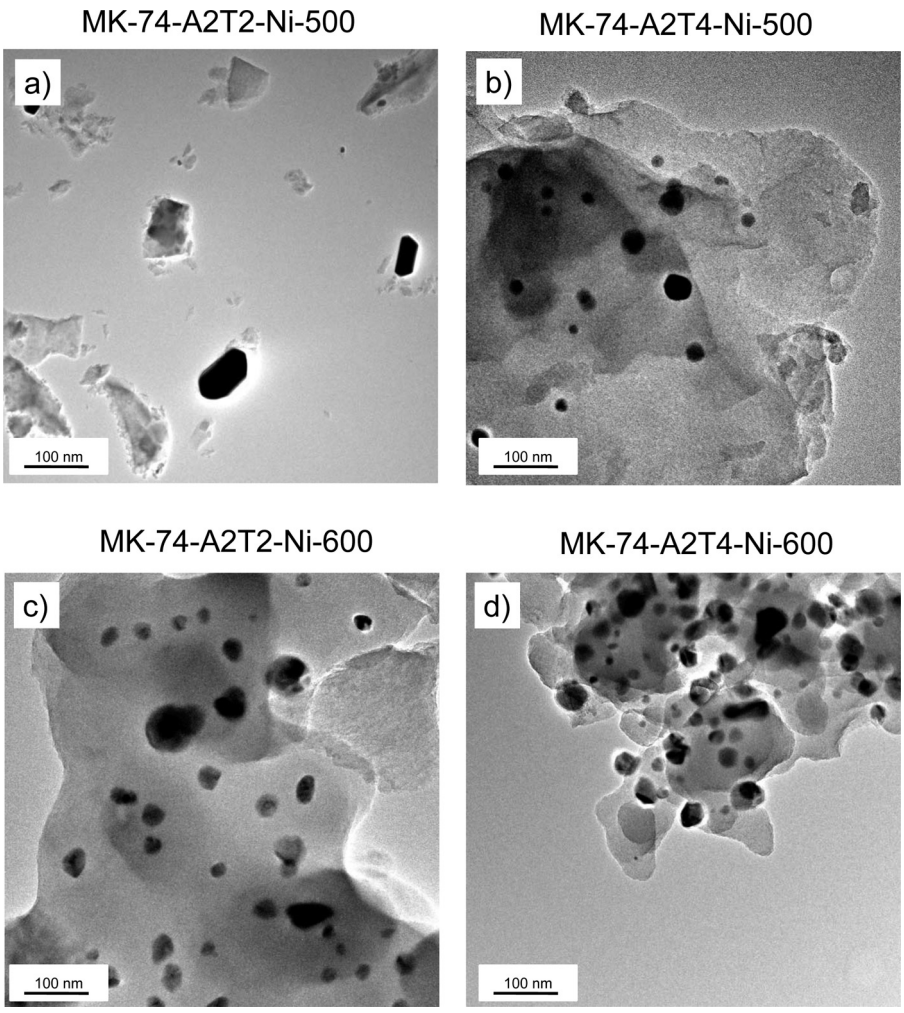

Fig. 3. TEM images of pyrolyzed Ni-containing monoliths with different precursor ratios (top: samples pyrolyzed at 500 °C, bottom: samples pyrolyzed at 600 °C).

3.2. Characterization at the microscopic length scale

Microporosity is important for realizing high specific surface areas; for adsorption of gases and vapors or educts in catalytic applications, for example. Micropores and mesopores were investigated by N_2 adsorption/desorption measurements, where type I isotherms are characteristic for microporous materials [35]. All MEBC and Ni-MEBC prepared in this study exhibit type I isotherms (not shown, see supplementary data) after pyrolysis indicating the pronounced microporosity of the materials. The specific BET surface areas (SSA) calculated from the nitrogen adsorption isotherms are shown in Fig. 5. The development of high SSAs via micropore formation during pyrolysis at temperatures of 500 and 600 °C is clearly evident.

Fig. 5 demonstrates that the post-pyrolysis SSA is fairly dependent on the different emulsion types for samples prepared with HIPEs and LIPEs. LIPE samples with different amounts of APTES/TEOS are depicted in Fig. 5, left side. The LIPE samples show a constant high SSA of 350 m^2/g ($\pm$50 m^2/g) which is nearly independent of the pyrolysis temperature and composition. In contrast, the HIPE samples show an increasing SSA, from 100 to 550 m^2/g ($\pm$50 m^2/g), roughly proportional to APTES/TEOS amount for both pyrolysis temperatures. This influence of APTES and TEOS is much stronger for the HIPE samples pyrolyzed at 500 °C than for those pyrolyzed at 600 °C.

A consistently high SSA of 450 m^2/g ($\pm$50 m^2/g) for the Ni-HIPE samples (Fig. 5; right) is observed for both pyrolysis temperatures. This is in contrast to the HIPE samples, which show an increasing SSA with an increasing APTES/TEOS amount.

3.3. Surface characteristics

The surface characteristics of materials are important as the area of interaction with other materials, especially so in catalytic applications. Adsorption of solvent vapors having different polarities at 22 °C are used in order to characterize the surface properties of the MEBCs and Ni-MEBCs, as shown in Fig. 6. Water and *n*-heptane are used as polar and non-polar solvent benchmarks, respectively [36]. The uptakes are calculated with the SSA gained from N_2 adsorption (Fig. 5). In Fig. 6 the ratio of water and *n*-heptane of the maximum uptake of the vapors is shown for samples pyrolyzed at 500 °C and at 600 °C. Values higher than 1 indicate a higher water uptake and a stronger hydrophilic surface characteristic. Correspondingly, values below 1 reveal a higher uptake of *n*-heptane, and the samples have a more hydrophobic surface characteristic.

All samples generally adsorb more *n*-heptane vapor than water vapor, so that the analyzed MEBCs and Ni-MEBCs have a higher affinity to non-polar vapors and with that a more hydrophobic surface characteristic (with the exception of Ni-MEBCs pyrolyzed at 600 °C). For the LIPE (Fig. 6, left), as well as the HIPE samples (Fig. 6, center), an increasing hydrophilic character with an increasing APTES/TEOS amount can be observed. This surface characteristic appears to be strongly dependent on the APTES/TEOS components in the LIPE samples. Different precursor composi-

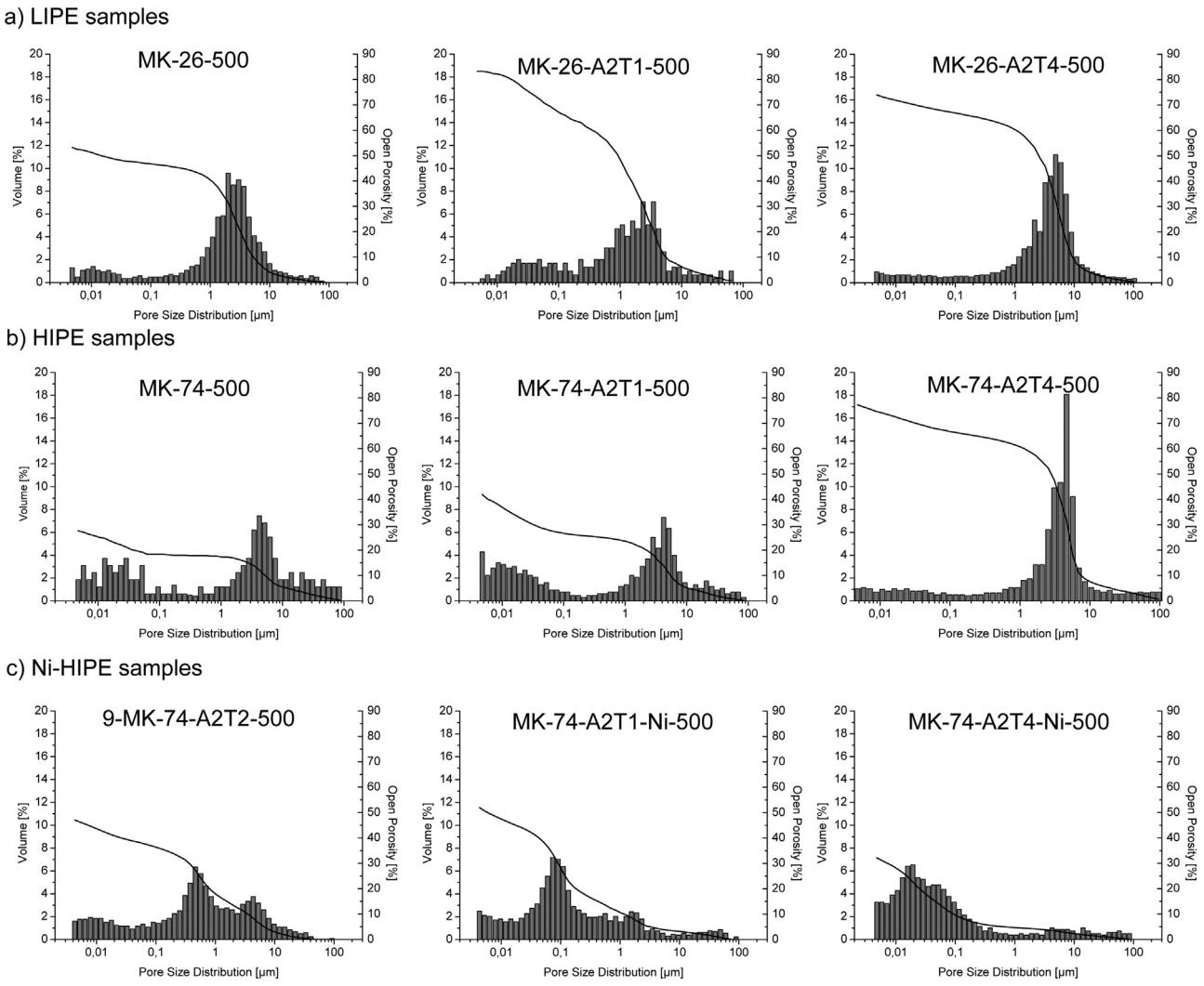

Fig. 4. Pore size distribution versus relative pore volume and open porosity curves obtained from Hg-porosimetry of pyrolyzed samples: (a) LIPE samples with different precursor ratios, pyrolyzed at 500 °C; (b) HIPE samples with different precursor ratios, pyrolyzed at 500 °C; (c) 9-MK-74-A2T2-500 and Ni-HIPE samples with different precursor ratios, pyrolyzed at 500 °C.

tions lead to different uptakes of water and *n*-heptane vapor for the LIPE samples pyrolyzed at 500 and 600 °C (Fig. 6, left). A strongly increasing hydrophilic character is observed with increasing amounts of APTES/TEOS. The HIPE samples, on the other hand, display only a slight increase in hydrophilicity with the increasing amount of APTES/TEOS. Different pyrolysis temperatures do not influence these surface characteristics strongly. The pyrolysis temperature had an entirely different effect on the Ni-MEBC samples' surface characteristics. Ni-HIPE samples pyrolyzed at 500 °C display a hydrophobic character; in agreement with Ni-free MEBC samples. Ni-MEBCs pyrolyzed at 600 °C display a substantially stronger hydrophilic character than comparable MEBC samples (Fig. 6, right).

4. Discussion

The generation of materials with a tailorable pore size distribution, high specific surface areas, tailorable surface characteristics in terms of hydrophobicity/hydrophilicity and the generation of metal nanoparticles is essential for the potentially application in catalysis. These tailorable characteristic can be achieved by preparing materials with a high content of different organic groups in the cross-linked state. Additionally, the incorporation of Ni in the MEBC

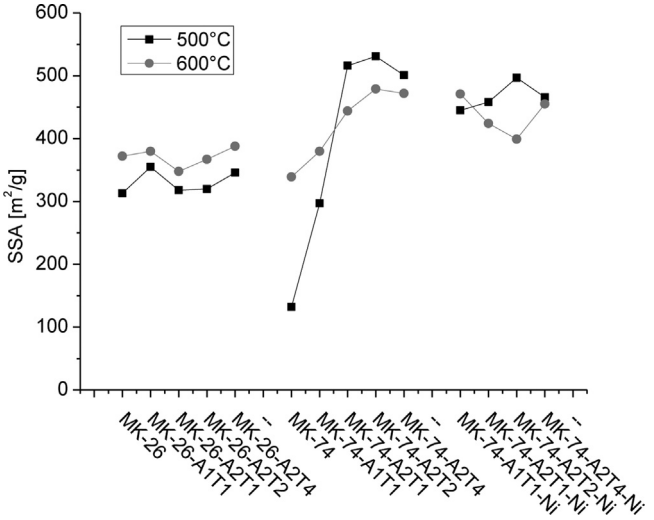

Fig. 5. Specific BET surface areas of pyrolyzed (500/600 °C) monoliths as determined by nitrogen adsorption for LIPE samples with different precursor ratios (left), for HIPE samples with different precursor ratios (center) and for Ni-HIPE samples (right).

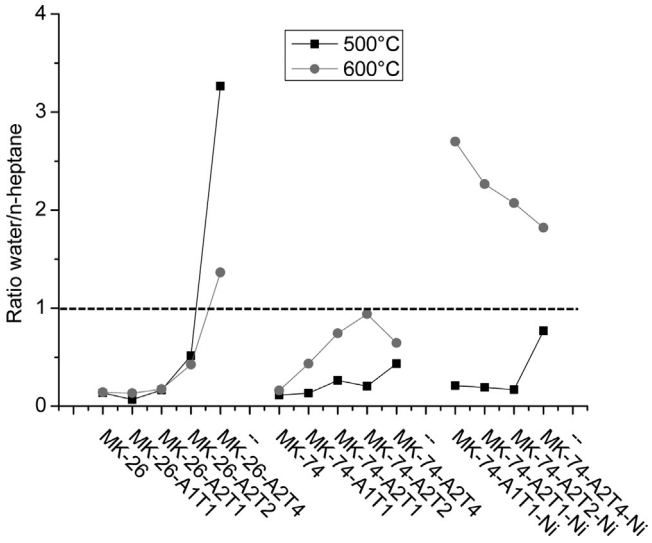

Fig. 6. Ratio of max. water and *n*-heptane vapor adsorption and desorption at 22 °C for LIPE samples with different precursor ratios (left), for HIPE samples with different precursor ratios (center) and for Ni-HIPE samples (right); pyrolyzed in both cases at 500 and 600 °C. The sorption data were recalculated using the specific BET surface area from N_2 adsorption shown in Fig. 4.

show the possibility to generate catalytic active materials in a one-pot synthesis. The monolithic structure of these emulsion based ceramers can be achieved with MK, APTES and TEOS as precursors. The material properties will be discussed in detail below.

4.1. Tailoring of macro and mesostructure and embedding of nickel nanoparticles

Materials based on pure MK (MK-26-500, MK-74-500, Fig. 2a and c) show the morphology of aggregated hollow spheres. The LIPE samples show a more polydisperse behavior, which results in sphere sizes between 5–25 μm. This polydisperse behavior can be also found in mercury intrusion experiments. By using different types of emulsions, for example LIPEs, a broad pore size distribution is obtained (Fig. 4a), which correlates with the SEM analysis. In the case of a polydisperse nature of the spheres the interstitial porosity, which is actually measured by the mercury intrusion, results in a broad pore size distribution. Instead of this smaller sphere sizes and a more monodisperse behavior (1–10 μm) were obtained for the HIPE samples. This is also in agreement with the mercury intrusion analysis. The interstitial porosity is more monodisperse if the spheres are more monodisperse. Smaller maximum diameters were found for the HIPE samples (around 0.01 μm and 4 μm, Fig. 4b).

Using LIPEs the internal oily phase has an amount of only 26 vol.% and what results in smaller and bigger oil droplets, when all other reaction conditions (e.g. same surfactant concentration or stirring velocity) are kept constant [2,4,37]. Using HIPEs the internal phase has an amount of 74 vol.%, so that many small oil droplets are formed, which might explain the different hollow sphere sizes and morphologies of the LIPE and HIPE samples. Since o/w emulsions were used the MK precursor was dissolved in the internal phase and with that the MK in oil droplets form a structure of aggregated spheres. Cross-linking of the polysiloxane MK starts at the oil/water interface and extends to the inner core of the oil droplet, which might be explain the building of aggregated hollow spheres [21,23]. The incorporation of APTES and TEOS leads to small particles distributed on the surface of hollow MK spheres. APTES and TEOS were dissolved in the aqueous, continuous phase and a so called "bicontinuous polymers" were created [2,4]. Hydrophobic precursor are dissolved in the oily apolar phase and the hydrophilic precursor in the aqueous phase. Probably MK cross-links together with APTES and TEOS so that APTES/TEOS is located on the surface of the MK hollow spheres (Fig. 2f).

The structure of Ni-MEBC differs from aggregated hollow sphere structure. Lower precursor concentrations (9 mol/L MK) results in a different macrostructure, compared to the samples prepared with 12 mol/L MK (Fig. 2a–d). The aggregated MK spheres with the residual APTES/TEOS decomposition products can be observed. This spheres are embedded in a larger foam-like [super]structure with pore sizes on the order of ~250 μm (Fig. 2e,f). This macrostructure occurs in all samples prepared with 9 mol/L MK – with and without Ni. The same results can be found in the mercury analysis. The Ni-HIPE samples show a broad monomodal pore size distribution between 0.004 and 0.2 μm (Fig. 4c). The second average cell size expected from SEM cannot be detected by this method, as mentioned before. This is in agreement with the SEM pictures (Fig. 2f), which demonstrated already that aggregated spheres are embedded in big pores (up to 250 μm). A similar foam structure (with unfilled cells) was previously observed by our group. The main difference of the Ni-MEBC and the other the MEBC is concentration of the precursor in oily respectively in the aqueous phase. A reason for the foam structure might be that due to the high amount of the oily internal phase (74 vol.%) the oil droplets might only be separated by a very thin continuous phase at the beginning. The cross-linking can start at the oil/water interface but due to the very thin water layers in between the chemical reaction proceeds as well to other oil droplets what results in a network with spherical pores. The macroscopic structure of Ni-MEBC looks like a combination of a foam structure and aggregated hollow sphere structure. These kind of structures were also observed for HIPE Pickering emulsions, the explanation of those structures is the same like given above [38]. It is also known, that different precursor and precursor concentrations results in different phase separation processes and surface tensions of the emulsions. The difference of the MK concentration might explain the different macroscopic textures of the samples. Especially the precursor concentration influence the cross-linking behavior very strong [3,39].

For many catalytic applications the metals should be dispersed as high as possible [40]. To analyze the particle size and local distribution of the nickel particles TEM investigations were done (Fig. 3a–d). Generally bigger nickel nanoparticles were found for Ni-MEBC prepared with a pyrolysis temperature of 500 °C (particle sizes up to 250 nm). For all the samples pyrolyzed at 600 °C nanoparticles in a range from 10–50 nm were observed, independent of APTES and TEOS amount and nickel content in the different samples. These particles were more homogeneously distributed in the matrix material (10–200 nm, Fig. 3b–d).

It is known from previously publications of our group that APTES, due to the amino groups, are able to complex the nickel ions [9,41]. Because of that and because APTES and $NiCl_2$ form a water soluble complex, we think that the nickel nanoparticles probably are located on the surface of the MK beads, as already discussed in macrostructure and SEM section. Additionally, we think that the accessibility of nickel nanoparticles should be very high for different gases or educts in catalytic applications.

The average particle sizes in the Ni-HIPEs, which were pyrolyzed at 600 °C, are in a range from 35 to 69 nm. As discussed before an important aspect for the generation of nickel nanoparticles with different sizes is the selection of metal precursor. Particles in a range from 3 to 82 nm are observed for $Ni(NO_3)_2$, $Ni(OAc)_2$, $NiCl_2$ and $Ni(acac)_2$. Smaller particles were received for $Ni(NO_3)_2$ and $Ni(OAc)_2$, bigger particles for $NiCl_2$ and $Ni(acac)_2$, which is in agreement with our results [17]. The bigger particles, which were generated at 500 °C, cannot be explained so far. Usually an increas-

ing metal particle size with an increasing pyrolysis temperature is observed [42].

4.2. Tailoring of microstructure

The HIPE samples show an increasing surface area from 100 to 550 m^2/g with an increasing APTES/TEOS amount for both pyrolysis temperatures (Fig. 5, center). A tailoring of the SSA of HIPE samples is possible by the incorporation of APTES and TEOS. It is known from previous works that APTES based materials generate more micropores than materials based on pure MK for pyrolysis temperature of 500 or 600 °C [43]. Because of that the resulting SSA is higher for APTES containing samples since the aminopropyl groups decompose at lower temperatures compared to the methyl groups. MK-74-500 show a SSA around 100 m^2/g, which is comparable to MK containing samples, which were cross-linked under reflux and pyrolyzed at 500 °C (SSA: ~100 m^2/g) [6,11]. By using higher amounts of APTES and TEOS higher SSA are observed, what can be explained on the one hand by the higher decomposition degree of APTES what results in a higher amount of micropores [9,10,43,44]. On the other hand TEOS exhibits four ethoxy groups that can cross-link and so the polysiloxane network will be strengthen and high SSA will be generated. This demonstrates that a tailoring of the SSA of HIPE samples is possible by the incorporation of APTES and TEOS.

A constant specific surface area around 350 m^2/g for samples pyrolyzed at 500 and 600 °C is observed for the LIPE samples. A relative high amount of TTAB (LIPE samples 1.62 g; HIPE samples 0.57 g) is used for the generation of the LIPE. It is known from previously publications of our group that the decomposition of TTAB also creates micropores and with that relative high SSA. Therefore the SSA of the LIPE samples is mainly generated by the decomposition of the surfactant TTAB and not by the precursor MK, APTES or TEOS.

For both pyrolysis temperatures the Ni-MEBC show a constant high SSA between 400 and 500 m^2/g (Fig. 5, right). This is in contrast to the HIPE samples, which show an increasing SSA with an increasing APTES/TEOS amount. It is known from the literature [9], that metals in a polysiloxane matrix can enhance the decomposition degree. Ni likely enhances the degree of decomposition for samples otherwise composed of pure MK, and for samples with low amounts of APTES and TEOS. With the higher decomposition degree more micropores might be generated and with that higher SSA are observed. Therefore high SSA are obtained samples made of pure MK and also for samples with low amounts of APTES and TEOS.

4.3. Surface characteristics

The surface characteristics of materials are important for interactions with, e.g. educts in catalytic applications. Solvent vapors of different polarity were used in order to characterize the surface of MEBC and Ni-MEBC, as shown in Fig. 6 for materials pyrolyzed at 500 and 600 °C.

Generally, hydrophobic materials were received, because high amounts of MK were used. MK shows a high decomposition temperature (~550 °C), so that many hydrophobic methyl groups remain in the final pyrolyzed material [43]. The HIPE samples show a just slightly increasing hydrophilic character with an increasing APTES and TEOS amount. In contrast to this, the incorporation of APTES and TEOS in the LIPE samples results in a strong increase of hydrophilic character. The more hydrophilic decomposition products of TEOS and APTES are located on surface of MK beads and are easy accessible (Fig. 2f). APTES show a higher degree of decomposition compared to MK at a pyrolysis temperature of 500 and 600 °C. In this way a higher content of SiO_2 domains in the final material is generated [43] and by this a higher affinity to water and a more hydrophilic character is achieved. Also, the use of TEOS influences the surface characteristics. An increasing TEOS amount results generally in an increasing hydrophilic character [11].

Ni-MEBC pyrolyzed at 600 °C show a strong hydrophilic character. Incorporation of Ni probably leads to a higher degree of precursor decomposition, leading to increases in the SiO_2 content of the final material. The surface characteristic, in terms of hydrophobicity/hydrophilicity, varies most strongly with changes in precursor composition and pyrolysis temperature.

MEBC and Ni-MEBC synthesized with polysiloxane precursor show a tailorable pore size distribution by using different emulsion types. Compared to Si(HIPE) [21–25] and R-Si(HIPE) [22,23,25,32] an introduction of organic groups up to 100% and the generation of monolithic structures at the same time is possible. With that, an adjustment of surface characteristic in terms of hydrophobicity/hydrophilicity and generation of high SSA is manageable. Additionally the incorporation of nickel by using complexing agents results in nickel nanoparticles (average particle size in a range from 35 to 69 nm for the samples pyrolyzed at 600 °C), which make the new material suitable for applications as catalyst.

5. Conclusion

Monolithic emulsion based ceramers with hierarchical porosity were obtained by using a HIPE or LIPE process, starting with siloxane precursors, which introduces a high amount of methyl and aminopropyl and ethoxy groups (MK, APTES, TEOS) in the samples. Three different siloxane precursor were used to generate materials with high content of different organic groups (>75 mol-%) in the cross-linked state. Nickel nanoparticles could be embedded successfully by using $NiCl_2$ together with the complexing agent APTES. Several characteristics like pore size distribution, SSA, surface characteristics in terms of hydrophobicity/hydrophilicity and size of the nickel nanoparticles of the investigated MEBC and Ni-MEBC can be specifically tailored. Using different types of emulsions (HIPEs or LIPEs) result in a controllable pore size distribution. The resulting hollow spheres, which consist of MK, were functionalized on the surface with the decomposition products of APTES and TEOS and exhibit different pore size distributions. The SSA and surface characteristics can be tailored by using different pyrolysis conditions or by selection of precursor and precursor combinations. Additionally, the incorporation of nickel leads to a tailorable SSA due to the higher decomposition degree. The pyrolysis of different precursor composition at 500 or 600 °C results in specific BET surface areas up to 550 m^2/g without losing the monolithic structure. Nickel nanoparticles in Ni-MEBC are generally well distributed and show metal nanoparticles in average particle size in a range from 35 to 69 nm for the samples pyrolyzed if the samples pyrolyzed at 600 °C. These materials possess a sufficient handling stability and high specific BET surface areas. Especially the Ni-MEBC is highly suitable for applications in catalysis. The supposed high accessibility of the nickel naonoparticles for different chemicals will be investigated in future studies.

Acknowledgements

This work was supported by the German Research Foundation (DFG) within the Research Training Group 1860 “Micro-, Meso- and Macroporous Nonmetallic Materials: Fundamentals and Applications”. Thorsten Mehrtens and Andreas Rosenauer are gratefully thanked for the recording of the TEM images.

Appendix A. Supplementary data

Supplementary data associated with this article can be found, in the online version, at http://dx.doi.org/10.1016/j.colsurfa.2015.12.020.

References

[1] N.R. Cameron, High internal phase emulsion templating as a route to well-defined porous polymers, Polymer 46 (2005) 1439–1449.
[2] I. Pulko, P. Krajnc, High internal phase emulsion templating—a path to hierarchically porous functional polymers, Macromol. Rapid Commun. 33 (2012) 1731–1746.
[3] C. Triantafillidis, M.S. Elsaesser, N. Hüsing, Chemical phase separation strategies towards silica monoliths with hierarchical porosity, Chem. Soc. Rev. 42 (2013) 3833–3846.
[4] M.S. Silverstein, Emulsion-templated porous polymers: a retrospective perspective, Polymer 55 (2014) 304–320.
[5] K. Terauds, P.E. Sanchez-Jimenez, R. Raj, C. Vakifahmetoglu, P. Colombo, Giant piezoresistivity of polymer-derived ceramics at high temperatures, J. Eur. Ceram. Soc. 30 (2010) 2203–2207.
[6] T. Prenzel, T.L. de Macedo Guedes, F. Schlüter, M. Wilhelm, K. Rezwan, Tailoring surfaces of hybrid ceramics for gas adsorption—from alkanes to CO_2, Sep. Purif. Technol. 129 (2014) 80–89.
[7] M. Wilhelm, C. Soltmann, D. Koch, G. Grathwohl, J. Eur. Ceram. Soc. 25 (2005) 271.
[8] T. Prenzel, M. Wilhelm, K. Rezwan, Pyrolyzed polysiloxane membranes with tailorable hydrophobicity, porosity and high specific surface area, Microporous Mesoporous Mater. 169 (2013) 160–167.
[9] M. Adam, M. Wilhelm, G. Grathwohl, Polysiloxane derived hybrid ceramics with nanodispersed Pt, Microporous Mesoporous Mater. 151 (2012) 195–200.
[10] M. Wilhelm, C. Soltmann, D. Koch, G. Grathwohl, Ceramers—functional materials for adsorption techniques, J. Europ. Ceram. Soc. 25 (2005) 271–276.
[11] H. Zhang, M. Wilhelm, K. Rezwan, Hierarchically ordered micro/meso/macroporous polymer derived ceramic monoliths fabricated by freeze-casting, J. Eur. Ceram. Soc. 36 (1) (2016) 51–58.
[12] P. Sonström, M. Adam, X. Wang, M. Wilhelm, G. Grathwohl, M. Bäumer, Colloidal nanoparticles embedded in ceramers: toward structurally designed catalysts, J. Phys. Chem. C 114 (2010) 14224–14232.
[13] M. Wilhelm, M. Adam, M. Bäumer, G. Grathwohl, Synthesis and properties of porous hybrid materials containing metallic nanoparticles, Adv. Eng. Mater. 10 (2008) 241–245.
[14] L.N.H. Arakaki, M.G. da Fonseca, E.C. da Silva Filho, A.P.M. de Alves, K.S. de Sousa, A.L.P. Silva, Extraction of Pb(II), Cd(II), and Hg(II) from aqueous solution by nitrogen and thiol functionality grafted to silica gel measured by calorimetry, Thermochim. Acta 450 (2006) 12–15.
[15] A. Gorschinski, G. Khelashvili, D. Schild, W. Habicht, R. Brand, M. Ghafari, H. Bonnemann, E. Dinjus, S. Behrens, A simple aminoalkyl siloxane-mediated route to functional magnetic metal nanoparticles and magnetic nanocomposites, J. Mater. Chem. 19 (2009) 8829–8838.
[16] A.M. Liu, K. Hidajat, S. Kawi, D.Y. Zhao, A new class of hybrid mesoporous materials with functionalized organic monolayers for selective adsorption of heavy metal ions, Chem. Commun. (2000) 1145–1146.
[17] G. Trimmel, C. Lembacher, G. Kickelbick, U. Schubert, Sol–gel processing of alkoxysilyl-substituted nickel complexes for the preparation of highly dispersed nickel in silica, New J. Chem. 26 (2002) 759–765.
[18] N. Brun, S. Ungureanu, H. Deleuze, R. Backov, Hybrid foams, colloids and beyond: from design to applications, Chem. Soc. Rev. 40 (2011) 771–788.
[19] N. Brun, S. Ungureanu, F. Carn, B. Julian-Lopez, R. Backov, Hybrid foams, colloids and beyond: advanced ceramics through integrative chemistry, Adv. Sci. Technol. (Stafa-Zuerich, Switzerland) 63 (2010) 97–106.
[20] C. Vakifahmetoglu, M. Balliana, P. Colombo, Ceramic foams and micro-beads from emulsions of a preceramic polymer, J. Eur. Ceram. Soc. 31 (2011) 1481–1490.
[21] F. Carn, A. Colin, M.F. Achard, H. Deleuze, E. Sellier, M. Birot, R. Backov, J. Mater. Chem. 14 (2004) 1370.
[22] S. Ungureanu, M. Birot, G. Laurent, H. Deleuze, O. Babot, B. Julian-Lopez, M.-F. Achard, M.I. Popa, C. Sanchez, R. Backov, One-pot syntheses of the first series of emulsion based hierarchical hybrid organic–inorganic open-cell monoliths possessing tunable functionality (organo-Si(HIPE) series), Chem. Mater. 19 (2007) 5786–5796.
[23] S. Ungureanu, H. Deleuze, C. Sanchez, M.I. Popa, R. Backov, First Pd@organo-Si(HIPE) open-cell hybrid monoliths generation offering cycling heck catalysis reactions, Chem. Mater. 20 (2008) 6494–6500.
[24] N. Brun, S.R.S. Prabaharan, M. Morcrette, C. Sanchez, G. Pecastaings, A. Derre, A. Soum, H. Deleuze, M. Birot, R. Backov, Hard macrocellular silica Si(HIPE) foams templating micro/macroporous carbonaceous monoliths: applications as lithium ion battery negative electrodes and electrochemical capacitors, Adv. Funct. Mater. 19 (2009) 3136–3145.
[25] S. Ungureanu, G. Laurent, H. Deleuze, O. Babot, M.F. Achard, M.I. Popa, C. Sanchez, R. Backov, Syntheses and characterization of new organically grafted silica foams, Colloids Surf. A 360 (2010) 85–93.
[26] A. Imhof, D.J. Pine, Uniform macroporous ceramics and plastics by emulsion templating, Chem. Eng. Technol. 21 (1998) 682–685.
[27] S.S. Manley, N. Graeber, Z. Grof, A. Menner, G.F. Hewitt, F. Stepanek, A. Bismarck, New insights into the relationship between internal phase level of emulsion templates and gas–liquid permeability of interconnected macroporous polymers, Soft Matter 5 (2009) 4780–4787.
[28] W. von Bonin, H. Bartel, Polymerization of vinyl compounds in water-in-oil emulsions, (Farbenfabriken Bayer A.-G.). Application: DE, DE, 1962, p. 4.
[29] H. Zhang, A.I. Cooper, Synthesis and applications of emulsion-templated porous materials, Soft Matter 1 (2005) 107–113.
[30] W.D. Bancroft, J. Phys. Chem. 17 (1913) 501–520.
[31] W.J. Griffin, Classification of surface-active agents by by HLB, J. Soc. Cosmet. Chem. 1 (1949) 311–321.
[32] N. Brun, B. Julian-Lopez, P. Hesemann, G. Laurent, H. Deleuze, C. Sanchez, M.-F. Achard, R. Backov, Eu3 + @organo-Si(HIPE) macro-mesocellular hybrid foams generation: syntheses, characterizations, and photonic properties, Chem. Mater. 20 (2008) 7117–7129.
[33] S. Ungureanu, H. Deleuze, O. Babot, M.F. Achard, C. Sanchez, M.I. Popa, R. Backov, Palladium nanoparticles heterogeneous nucleation within organically grafted silica foams and their use as catalyst supports toward the Suzuki–Miyaura and Mizoroki–Heck coupling reactions, Appl. Catal. A 390 (2010) 51–58.
[34] J. Rouquerol, D. Avnir, C.W. Fairbridge, D.H. Everett, J.H. Haynes, N. Pernicone, J.D.F. Ramsay, K.S.W. Sing, K.K. Unger, Recommendations for the characterization of porous solids, Pure Appl. Chem. 66 (1994) 1739–1758.
[35] K.S.W. Sing, D.H. Everett, R.A.W. Haul, L. Moscou, R.A. Pierotti, J. Rouquerol, T. Siemieniewska, Reporting physisorption data for gas/solid systems with special reference to the determination of surface area and porosity (Recommendations 1984), Pure Appl. Chem. 57 (1985) 603–619.
[36] K. Stana-Kleinschek, V. Ribitsch, T. Kreze, L. Fras, Determination of the adsorption character of cellulose fibres using surface tension and surface charge, Mater. Res. Innov. 6 (2002) 13–18.
[37] C. Zhao, E. Danish, N.R. Cameron, R. Kataky, Emulsion-templated porous materials (PolyHIPEs) for selective ion and molecular recognition and transport: applications in electrochemical sensing, J. Mater. Chem. 17 (2007) 2446–2453.
[38] A. Menner, V. Ikem, M. Salgueiro, M.S.P. Shaffer, A. Bismarck, High internal phase emulsion templates solely stabilised by functionalised titania nanoparticles, Chem. Commun (2007) 4274–4276.
[39] C.J. Brinker, G.W. Scherer, Sol–gel Science: The Physics and Chemistry of Sol–gel Processing, Academic Press, 1990.
[40] S. Özkar, Enhancement of catalytic activity by increasing surface area in heterogeneous catalysis, Appl. Surf. Sci. 256 (2009) 1272–1277.
[41] M. Adam, C. Vakifahmetoglu, P. Colombo, M. Wilhelm, G. Grathwohl, Polysiloxane-derived ceramics containing nanowires with catalytically active tips, J. Am. Ceram. Soc. 97 (2014) 959–966.
[42] M. Zaheer, T. Schmalz, G. Motz, R. Kempe, Polymer derived non-oxide ceramics modified with late transition metals, Chem. Soc. Rev. 41 (2012) 5102–5116.
[43] M. Scheffler, T. Gambaryan-Roisman, T. Takahashi, J. Kaschta, H. Muenstedt, P. Buhler, P. Greil, Pyrolytic decomposition of preceramic organo polysiloxanes, Ceram. Trans. 115 (2000) 239–250.
[44] T. Prenzel, M. Wilhelm, K. Rezwan, Tailoring amine functionalized hybrid ceramics to control CO_2 adsorption, Chem. Eng. J. 235 (2013) 198–206.